The Korean Nuclear Society Spring Meeting
Jeju, Korea, May 22-23, 2025

Prototype Tracking Simulation for Nuclear Power Plant Dismantling Using a BIM-Based Radiation Model

Hyong Chol Kim*, Jae Hee Ro, Moonjoo Gil, Young Jin Lee

NSE TECHNOLOGY

Contents

『Prototype Tracking Simulation for Nuclear Power Plant Dismantling Using a BIM-Based Radiation Model』

1. Introduction

- Background
  - 3D modeling techniques have become widely utilized in the design, operation, and decommissioning of NPPs.
  - 3D model-based dose assessment programs have been developed to support the ALARA analysis in radiation work planning [EPRI, 2012].
  - For NPP decommissioning, radiological characterization is conducted to gather information on the type, quantity, and distribution of radionuclides within the facility.
  - A BIM-based program can be employed to determine the activity levels of radiation sources, enhancing both efficiency and safety in dismantling components and managing radioactive materials during decommissioning processes [A. H. Oti, et al. (2022)].
  - A virtual simulation system for radiation work processes is crucial in mitigating potential challenges and associated risks.
- Aims of the current study
  - BIM-based software program called BIMRAD was introduced.
  - BIMRAD is applied for tracking simulations during an NPP dismantling process and assessing the radiation field and radiation exposure.

2. Methods

2.1 Determination of Source Strength from Field-Measured Dose Rates (1/2)

- **Dose rate response (R_{mj}) from a unit point kerel source**
  - $$R_{mj} = \int_{V_j} \int_E \left\{ \frac{\chi(E) \cdot C(E) \cdot B(E, \mu T) \cdot e^{-\mu T}}{4\pi (r_j - r_m)^2} \right\} dE dV$$

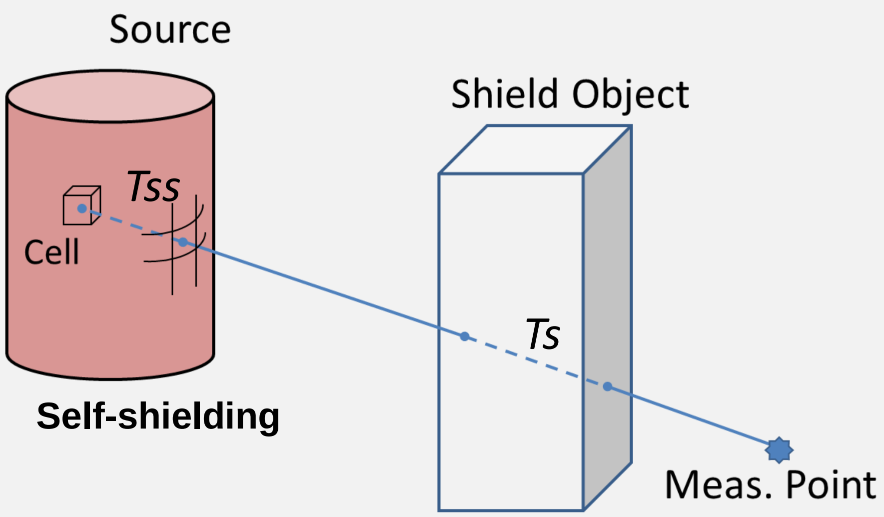

- **Path length determination**
  - **Shield path length (Ts) by pairs of points on the inlet and outlet surface meshes of shielding object models**
  - **Source object is represented as a phantom of equivalent simple geometrical shape which can be subdivided into multiple cells**
  - **Self-shielding length (Tss) is calculated algebraically by determining the intersection of the line extending from the center of each cell with the outer surface of the phantom**

2. Methods

2.1 Determination of Source Strength from Field-Measured Dose Rates (2/2)

- **Dose rate** (D_m) **from Source Strength** (S_j)

$$D_m = \sum_{j=1}^{N} \left[R_{mj} \cdot S_j \right] \ (m = 1, \cdots, M;\ M \geq N)$$

(1) Forward Eq.

  - *M = No. of measured dose rates*
  - *N = No. of sources*

- **Inverse equation set for** S_j **with LSE**

$$\sum_{j=1}^{N} \left[\left(\sum_{m=1}^{M} R_{mk} R_{mj} \right) \cdot S_j \right] = \sum_{m=1}^{M} \left[D_m R_{mk} \right] \quad (\mathrm{k}=1, \cdots, \mathrm{N}) \ (S_j \geq 0.)$$

(2) Inverse Eq.

- **Total Activity** (A_j) **of source** ***j***

(3) Activity Eq.

$$A_j = S_j V_j.$$

2. Methods

2.2 Radiation Field and Exposure Estimation

- **Generation of the radiation field and the dose rate contour map**
  - S_j **obtained from Inverse Eq. (2)**
  - **Dose rates at arbitrary positions in the field can be evaluated by substituting S_j into Forward Eq.**

$$D_x = \sum_{j=1}^{N} \left[R_{xj} \cdot S_j \right]$$

(1') Forward Eq.

- **Radiation exposure dose = (dose rate;** D**) x (duration of exposure;** T**)**
- **Total dose exposure** (E)

$$E = \sum_{i=1}^{L} (D_i \cdot T_{wi}) + \sum_{i=2}^{L} \left[\frac{(D_{i-1} + D_i)}{2} \cdot T_{ti} \right],$$

(4) Exposure Eq.

  - L = *number of working positions,*
  - T_{wi} = *work time at position i, and*
  - T_{ti} = *travel time between positions i-1 and i.*

3. Tracking Simulation

3.1 Test Scene Description (1/2)

- **Scene Description**
  - **Area : ~ 100 m^2**
  - **Vertical Pipe Sources:**
    - **10 cm ID and 20cm OD with a length of 1 m**
    - **arranged in a row at 2 m intervals along the x-direction**
    - **centered on the imaginary x-y plane and labeled S-1 through S-5**
  - **Horizontal Transverse Pipe Sources:**
    - **measuring 2 m in length**
    - **labeled S-6 and S-7**
  - **Shielding:**
    - **concrete wall of 20cm x 5 m x 5 m**
    - **labeled W-8.**
  - **Measurement points:**
    - **labeled P1 through P10**

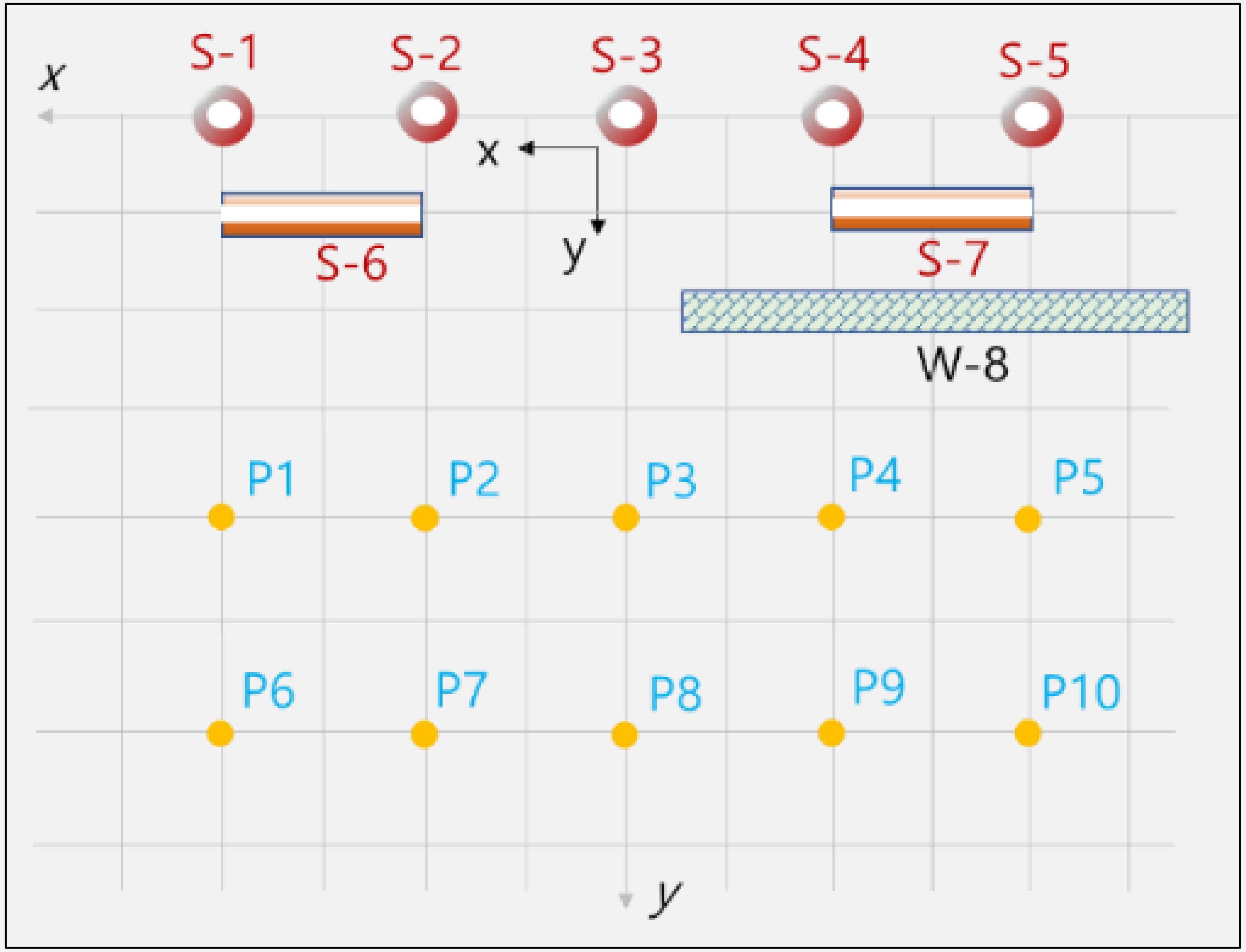

Fig. 1. Planar layout of the test radiation scene.

3.1 Test Scene Description (2/2)

- **BIMRAD 3D model of the scene**
  - **Radiation sources are highlighted in red,**
  - **Shielding wall is displayed in dark green,**
  - **Measurement points represented in yellow.**

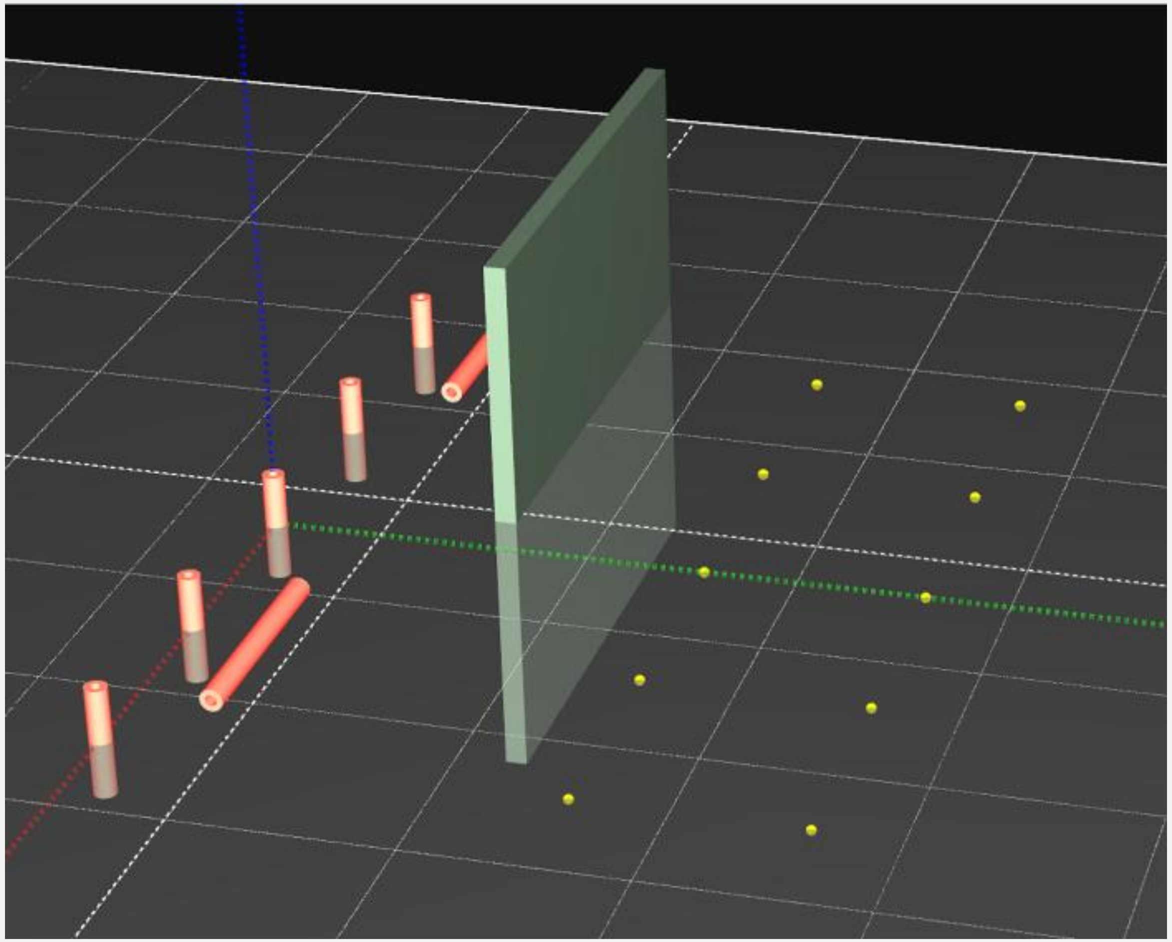

Fig. 2. 3D image of the test scene with the measurement points displayed on an imaginary plane.

3.2 Measured Dose Rates and Source Strength Estimation (1/2)

- **Sources**
  - **Co-60 steel**
  - **Strengths in LLW range**
  - **Higher strengths to the shielded sources**

Assigned source strength

Sources	S-1	S-2	S-3	S-4	S-5	S-6	S-7
Source Strength (MBq/cm^3)	3	5	8	10	20	5	10

- **Dose rates at measurement points**
  - **determined by MCNP**

Table I: Dose rates at the measurement points.

Meas. Points	**P1**	**P2**	**P3**	**P4**	**P5**
Dose rates ($\mu Sv/hr$)	5299.5	5357.8	3633.9	2273.5	1620.1
Meas. Points	**P6**	**P7**	**P8**	**P9**	**P10**
Dose rates ($\mu Sv/hr$)	2236.9	2117.0	1993.1	1316.5	1056.6

3.2 Measured Dose Rates and Source Strength Estimation (2/2)

- **Source strength estimation by BIMRAD**
  - **Source modeling**
    - **Vertical pipes: 1x4x4 cells in (r,θ,l)**
    - **Horizontal pipes: 1x4x8 cells in (r,θ,l)**
  - **Estimation error ≤ ±40%**

Table II: Estimation results of the source strengths.

Sources	S-1	S-2	S-3	S-4	S-5	S-6	S-7
Given	3	5	8	10	20	5	10
Estimated	3.11	5.63	11.18	12.92	27.61	5.10	9.08
Error (%)	+3.7	+12.6	+36.7	+29.2	+38.0	+2.1	-9.2

(Unit: MBq/cm^3)

  - **Comparable to the 50% uncertainty recorded in similar applications [H. Toubon, et al., 2011]**
  - **Total radioactivity inventory can be calculated by summing up activities of $A_j = S_j V_j$.**

3. Tracking Simulation

3.3 Construction of the Initial Radiation Field (1/3)

- **Radiation contour map by BIMRAD**
  - **Forward Eq. (1) is used for arbitrary points x from the estimated source strengths.**

$$D_x = \sum_{j=1}^{N} \left[R_{xj} \cdot S_j \right]$$

  - **Contour lines can be shown for a selected dose rate.**
  - **Dose rates and coordinates can be shown for cursor positions.**

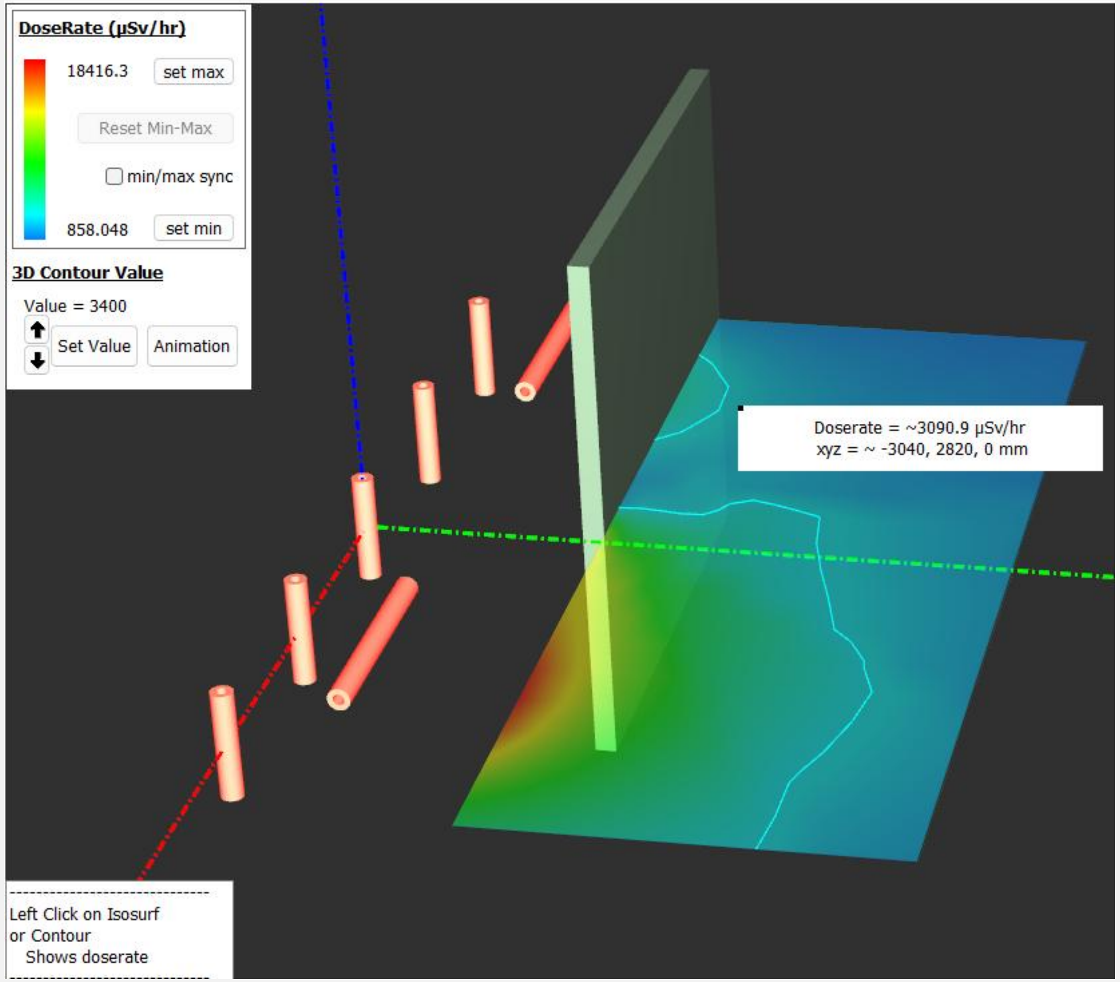

Fig. 3. Radiation contour map of the test scene generated by BIMRAD.

3.3 Construction of the Initial Radiation Field (2/3)

- **Confirmation of radiation field**
  - **Dose rates re-calculated by BIMRAD at measurement points**
  - **Re-calculated dose rate error ≤ ±10%**
  - **Ref: Acceptable uncertainty threshold for industry vendors is 50% [EPRI, 2012]**

Table III: Re-calculated dose rates compared to the measured

Meas. Points	P1	P2	P3	P4	P5
Re-calculated ($\mu Sv/hr$)	4850.	5347.	3988.	2499.	1624.
Error (%)	-8.5	-0.20	9.8	10.0	0.25
Meas. Points	P6	P7	P8	P9	P10
Re-calculated ($\mu Sv/hr$)	2150.	2123.	2089.	1449.	1143.
Error (%)	-3.8	0.32	4.8	10.1	8.2

3.3 Construction of the Initial Radiation Field (3/3)

- **Radiation work exposure estimation**
  - **Work path drawn on the scene**
  - **Estimated radiation exposure for the path is 22,099 μSv by using Exposure Eq. (4).**
  - **Work time at each point on the path was assumed to be 60 minutes, with no travel time considered between work positions.**

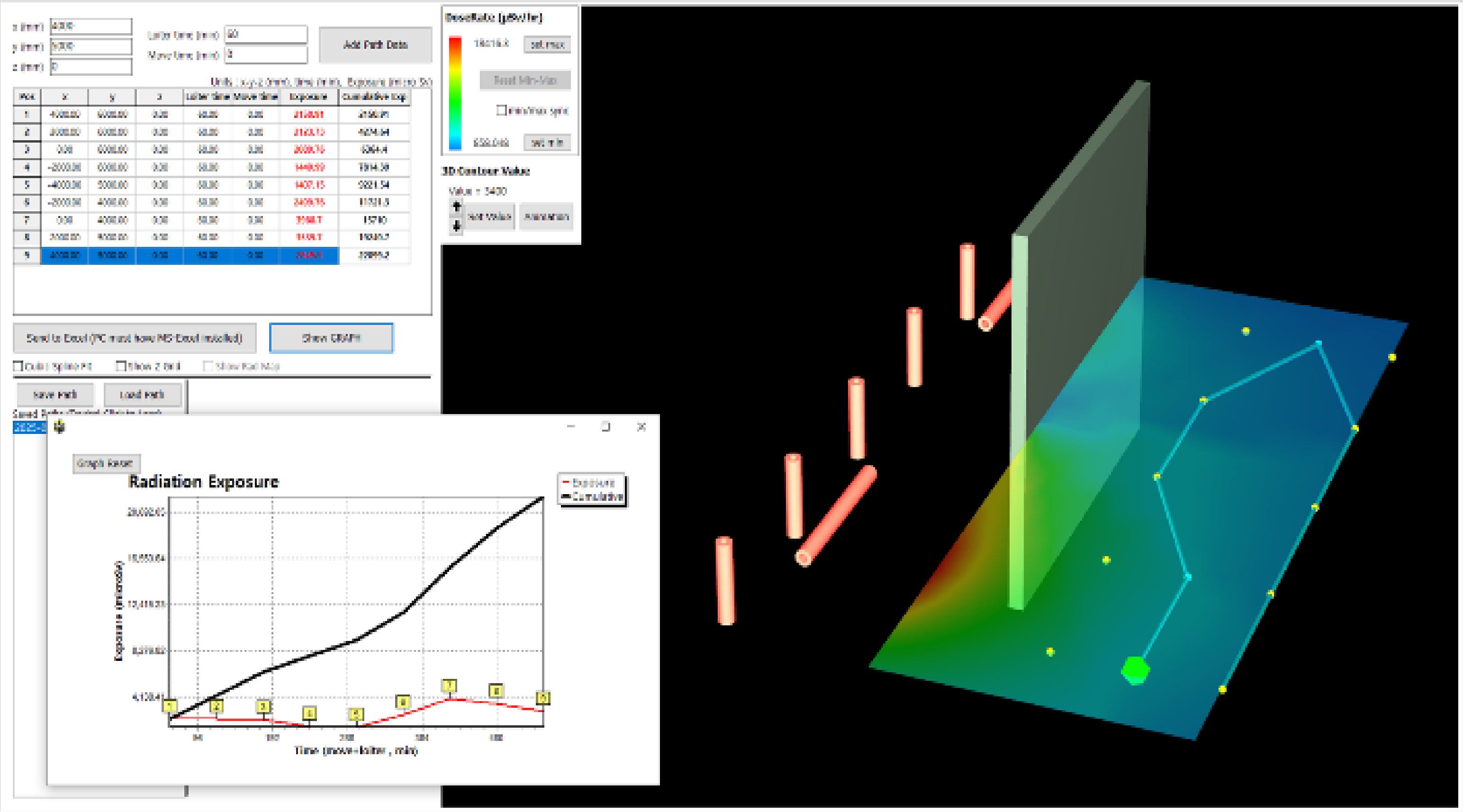

Fig. 4. A radiation work path and the associated radiation exposure graph.

3. Tracking Simulation

3.4 Dismantling Tracking (1/4)

- The color of the source changes from red to gray when the sources are selected for dismantling.
- As the dismantling of radiation sources progresses, the radiation field undergoes corresponding changes.
- The contour map illustrates the range of dose rates within the designated display area, allowing for a quantitative evaluation of dose rate changes in the radiation field.
- The area enclosed by a contour line diminishes as dismantling progresses.
- This change in the radiation field can be evaluated without requiring direct dose rate measurements at each dismantling stage.

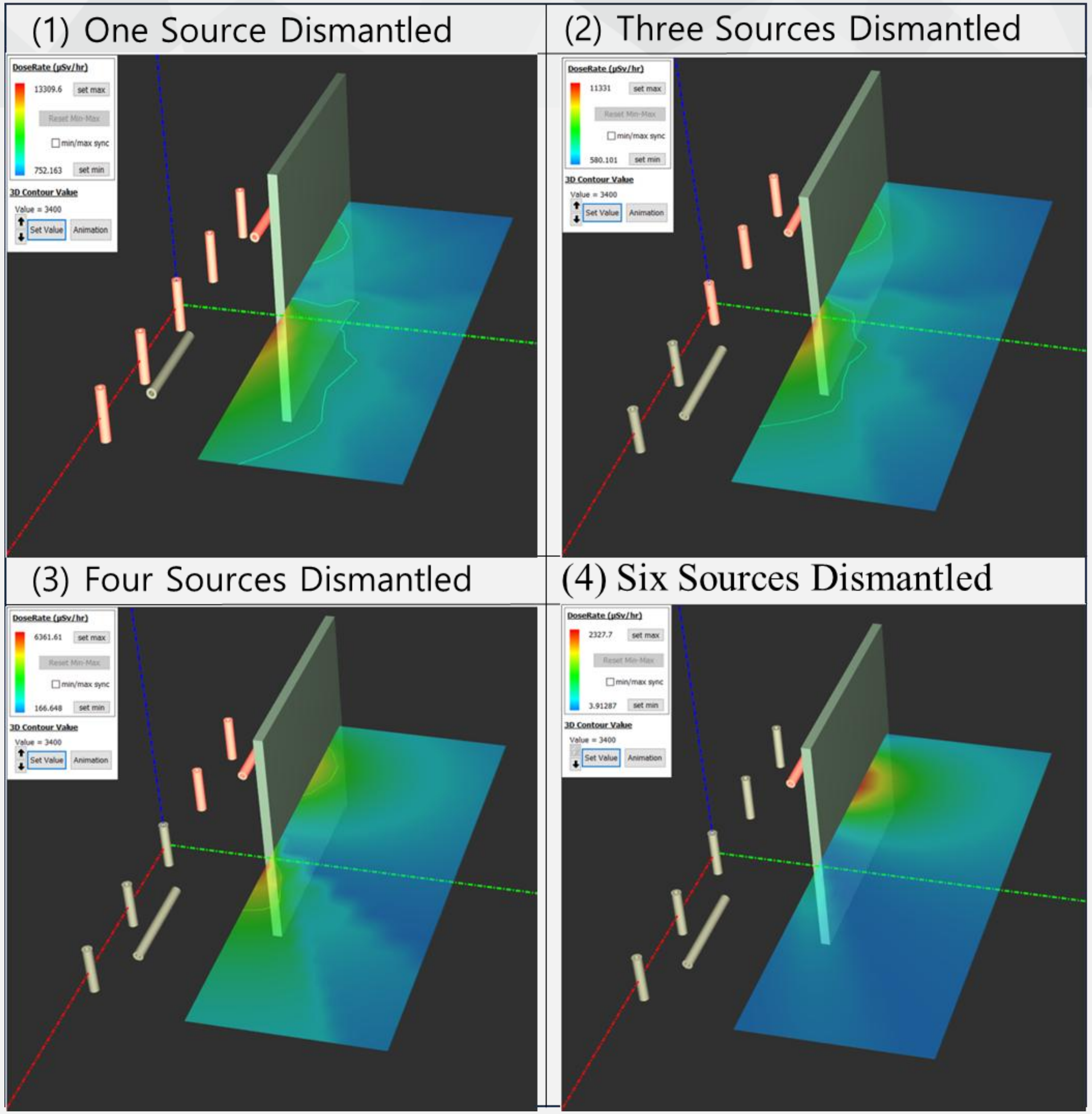

Fig. 5. Radiation field change in accordance with source dismantling.

3. Tracking Simulation

3.4 Dismantling Tracking (2/4)

- **BIMRAD offers a three-dimensional contour surface display option.**
- **Fig.6 shows a 3D contour surface representing the dose rate at half value in the last phase.**

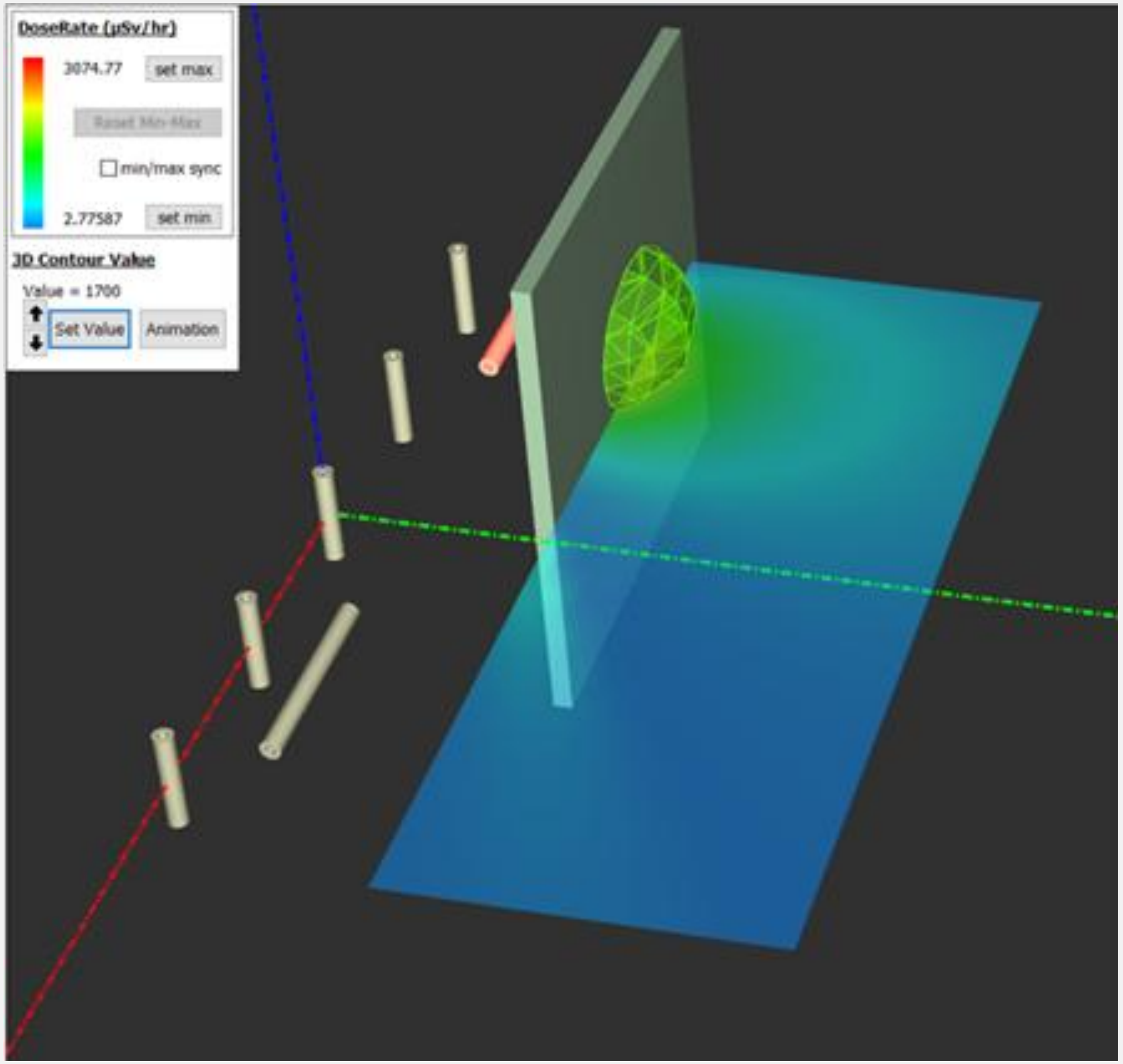

Fig. 6. An example of 3D Radiation contour surface.

3.4 Dismantling Tracking (3/4)

- **BIMRAD can assess the effects of shielding objects.**
- **Fig. 7 depicts the radiation contour map generated by BIMRAD when the shielding wall is assumed to be removed in the last phase.**
- **In this scenario, the shielding wall changes to semi-transparent gray, and the area with a dose rate exceeding a given value becomes larger.**

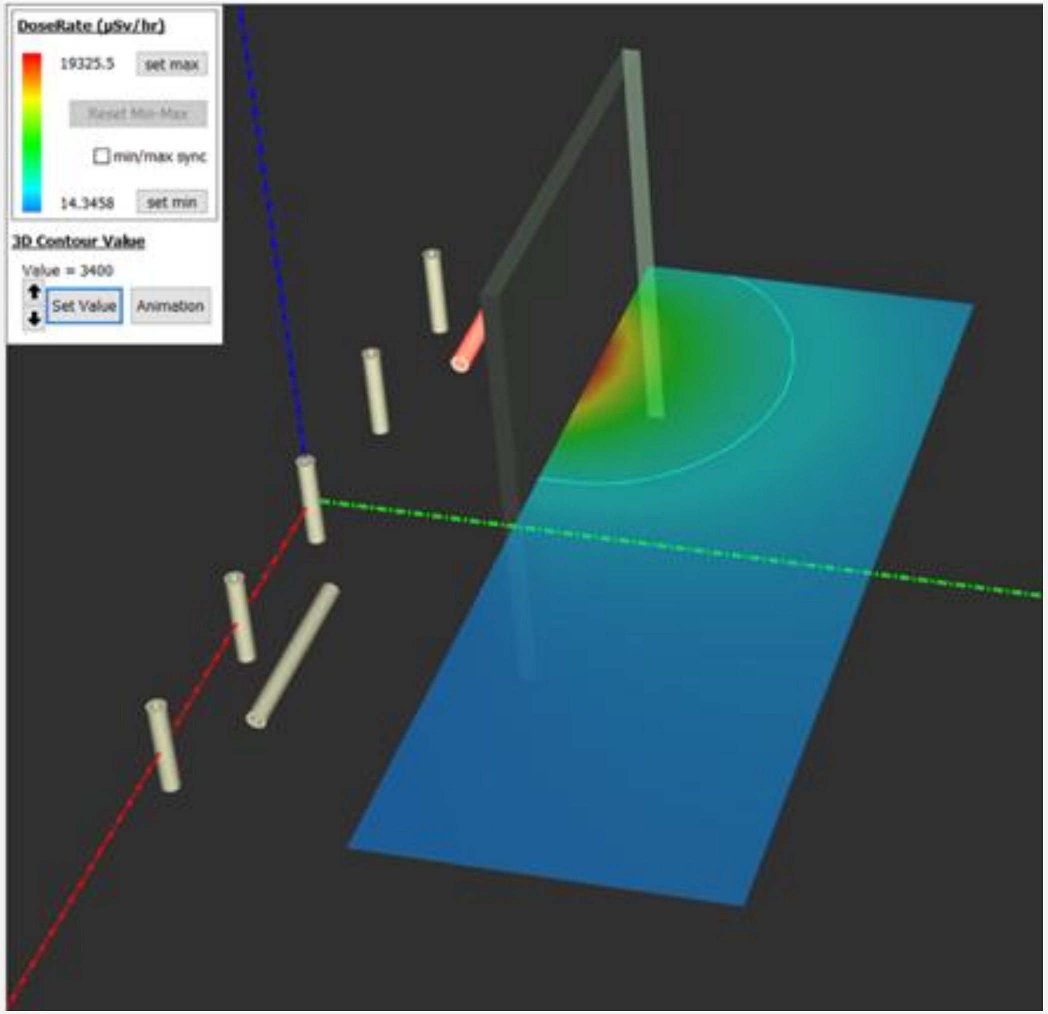

Fig. 7. The radiation contour map when the shielding wall is removed

3. Tracking Simulation

3.4 Dismantling Tracking (4/4)

- **Fig.8 presents the results of radiation exposure evaluations for a work path with the shielding wall and without it.**
- **The work path is the same as the initial stage of Fig. 4, but now it involves only one radiation source.**
- **The estimated radiation exposure from the work is 1,431 μSv when the shielding wall is retained,**
- **whereas it increases to 12,319 μSv when the shielding wall is removed.**

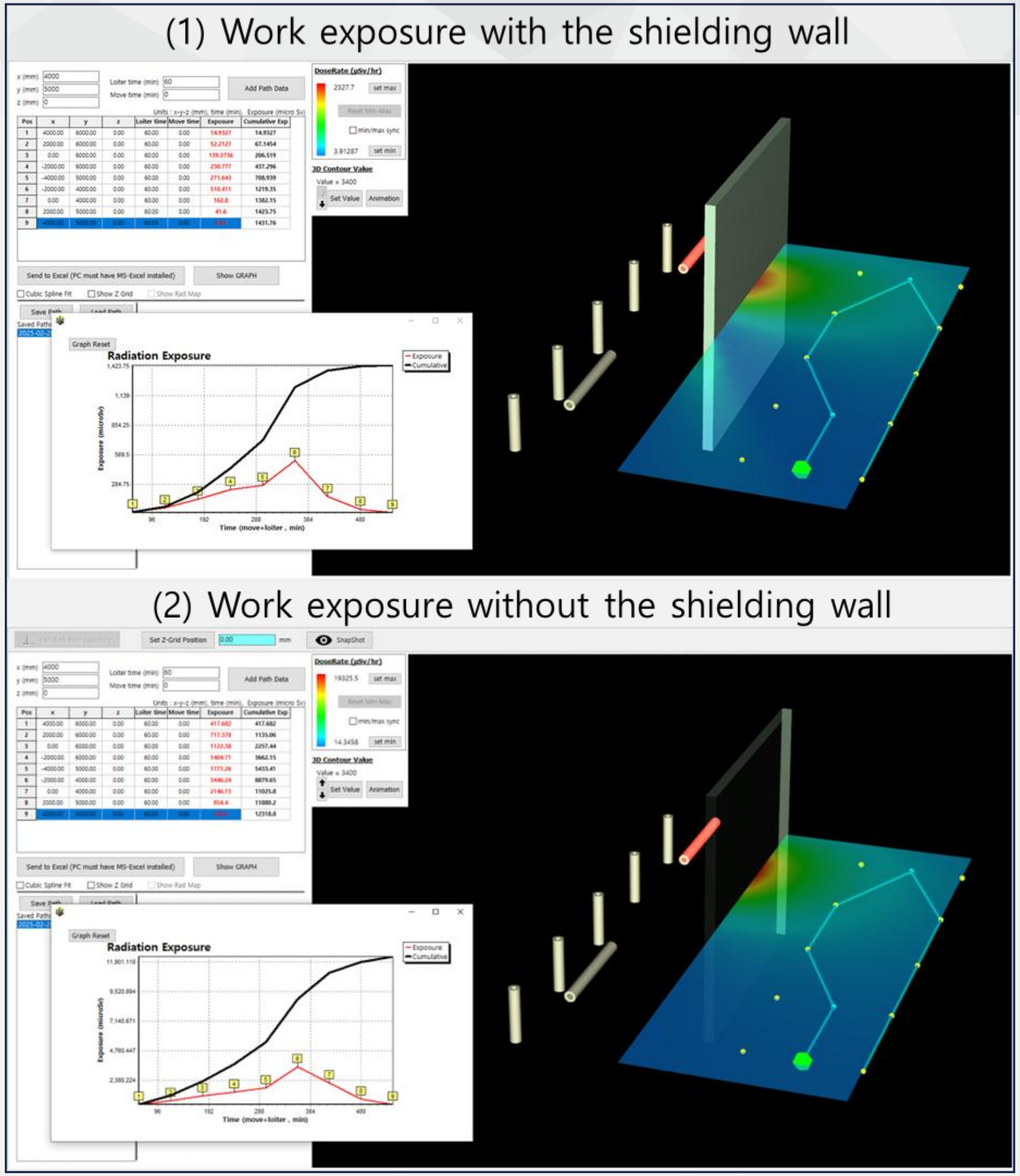

Fig. 8. Comparison of radiation exposures with and without the shielding wall.

4. Conclusions

- A BIM-based software tool has been developed to estimate radiation source strengths using field-measured dose rates. This tool is designed to support the estimation of radioactivity inventory distribution for NPP decommissioning planning.
- BIMRAD provides 3D dose rate distributions, valuable for ALARA analyses in radiation work planning.
- The estimation accuracy for source strengths is approximately ±40%, while the accuracy for dose rates within the radiation field is well within ±20%. These accuracy levels are considered comparable to industry convention.
- BIMRAD can evaluate dose rate and exposure changes as dismantling proceeds, while offering 3D visualizations to enhance understanding of the radiation field. This tracking simulation is conducted without requiring additional dose rate measurements at each dismantling stage, once source strengths are determined from initial stage measurements.
- The tool can also be utilized to evaluate various alternatives for component dismantling and work planning during NPP decommissioning by leveraging BIMRAD's functionality to either retain or remove sources and shielding objects.
- Although the accuracy of the estimations may vary depending on the geometrical complexity of the scene and the precision of dose rate measurements, BIMRAD's methodology is a valuable resource for inventory estimation and exposure analysis during dismantling.

  

ACKNOWLEDGEMENTS

This work was conducted under the project titled ‘Development of radiation safety diagnosis platform based on synchronization of digital coordinates and radioactivity information of facilities in NPP’ (No. 20217910100130) supported by KETEP and MOTIE.

nse
TECHNOLOGY